Wang *et al.*
Journal of NeuroEngineering and Rehabilitation (2024) 21:177
https://doi.org/10.1186/s12984-024-01466-y

Journal of NeuroEngineering and Rehabilitation

RESEARCH

Open Access

Analysis of electrode locations on limb condition effect for myoelectric pattern recognition

Hai Wang[1,2,3], Na Li[1,2,3], Xiaoyao Gao[1,2,3], Ning Jiang[1,2,3] and Jiayuan He[2,3*]

Abstract

Background Gesture recognition using surface electromyography (sEMG) has garnered significant attention due to its potential for intuitive and natural control in wearable human–machine interfaces. However, ensuring robustness remains essential and is currently the primary challenge for practical applications.

Methods This study investigates the impact of limb conditions and analyzes the influence of electrode placement. Both static and dynamic limb conditions were examined using electrodes positioned on the wrist, elbow, and the midpoint between them. Initially, we compared classification performance across various training conditions at these three electrode locations. Subsequently, a feature space analysis was conducted to quantify the effects of limb conditions. Finally, strategies for group training and feature selection were explored to mitigate these effects.

Results The results indicate that with the state-of-the-art method, classification performance at the wrist was comparable to that at the middle position, both of which outperformed the elbow, consistent with the findings from the feature space analysis. In inter-condition classification, training under dynamic limb conditions yielded better results than training under static conditions, especially at the positions covered by dynamic training. Additionally, fast and slow movement speeds produced similar performance outcomes. To mitigate the effects of limb conditions, adding more training conditions reduced classification errors; however, this reduction plateaued after four conditions, resulting in classification errors of 22.72%, 22.65%, and 26.58% for the wrist, middle, and elbow, respectively. Feature selection further improved classification performance, reducing errors to 19.98%, 19.75%, and 27.14% at the respective electrode locations, using three optimal features derived from single-condition training.

Conclusions The study demonstrated that the impact of limb conditions was mitigated when electrodes were placed near the wrist. Dynamic limb condition training, combined with feature optimization, proved to be an effective strategy for reducing this effect. This work contributes to enhancing the robustness of myoelectric-controlled interfaces, thereby advancing the development of wearable intelligent devices.

Keywords Myoelectric signals, Pattern recognition, Robustness, Limb conditions, Electrode placement

*Correspondence:
Jiayuan He
jiayuan.he@wchscu.cn
[1] Center of Gerontology and Geriatrics, West China Hospital of Sichuan University, Chengdu 610041, Sichuan, China
[2] Innovation Institute for Integration of Medicine and Engineering, West China Hospital of Sichuan University, Chengdu 610041, Sichuan, China
[3] The Med-X Center for Manufacturing, Sichuan University, Chengdu 610041, Sichuan, China

Background

Myoelectric control is widely utilized in prosthetic limb control, rehabilitation, robotics, and virtual reality due to its natural and intuitive control capabilities. A critical challenge in this field is achieving a robust and high-accuracy muscular human–machine interface [1]. Despite decades of advancements in myoelectric control, the primary goal remains to develop a dependable

interface for everyday use [2]. Initially, myoelectric control was employed to control the opening and closing of prosthetic hands. In 1948, Reiter et al. [3] pioneered the world's first prosthetic system controlled by sEMG (surface electromyography) recognition technology. However, the sEMG recognition technology of that era was quite rudimentary, offering only a limited number of control options. The ongoing development of sEMG intention-sensing technology promises to significantly enhance the performance of sEMG-controlled prosthetic hands, which will, in turn, greatly improve the quality of life for amputees [4]. With advancements in pattern recognition, scientists have developed systems for controlling multiple gestures and decoding continuous finger flexion angles. However, ensuring robustness remains essential and is currently the primary challenge for practical applications.

To improve the robustness of sEMG pattern recognition systems, researchers are exploring new methods to address challenges related to limb conditions and electrode placements. In particular, sEMG pattern recognition is significantly affected by variations in limb conditions and the positioning of sEMG electrodes. For limb conditions, Fougner et al. [5] explored gesture recognition ability under different limb conditions using five static limb positions and provided two solutions to improve robustness. Geng et al. [6] extended this work by extending the experiment in trans-radial amputees, where five static arm conditions were considered. For exploring the dynamic limb conditions' influence on gesture recognition, Liu et al. [7] adopted three metrics to quantify the changes of sEMG pattern characteristics change caused by the variation of limb conditions. For sEMG acquisition location, it influences the concrete information of sEMG. Thus, the comparison of different recognition performance in different locations' sEMG is very fundamental for the improvement of robustness. He et al. [8] use 8 equidistant electrodes on the forearm and 6 equidistant electrodes on the wrist to prove that wrist sEMG is better than forearm sEMG in gesture recognition. Botros et al. [9] use four electrodes in wrist and four in forearm level to compare their recognition ability. In the end, he proved that wrist sEMG has better effect on recognizing fine finger movements. Islam et al. [10] conducted a comprehensive study, finding that signals from the middle of the extensor digitorum communis and extensor digiti minimi muscles provide better signal quality and improved finger movement recognition. Other researchers have addressed similar challenges using multi-information fusion and machine learning models. For example, Pan et al. [11] combined eight-channel sEMG with inertial measurement units to achieve higher accuracy. Juan et al. [12] enhanced gesture classification robustness by employing reinforcement learning. Yamanoi et al. [13] developed a convolutional neural network (CNN) to improve classification robustness and reduce the impact of electrode position changes. Geng et al. [6] compared three strategies for enhancing system robustness and found that a cascade classifier, which first detects limb positions using accelerometers (ACC), was the most effective. In addition, researchers have explored various artificial intelligence models to enhance pattern recognition robustness. A selective classification approach, integrating different machine learning techniques under clinical conditions, has been proposed to improve gesture recognition robustness [14]. Traditional machine learning methods, including multiple regression [15], Gaussian process regression [16], and neural networks [17], are frequently used for continuous angle decoding. Ensemble learning pipelines have also been introduced to further boost performance [18]. For deep learning, several models have been applied to gesture recognition tasks. These include Convolutional Neural Networks (CNNs) [19], Recurrent Neural Networks (RNNs), autoencoders (AE), Deep Forest models [20], and deep transfer learning [21]. Bao et al. [22] combined CNNs with Long Short-Term Memory (LSTM) networks to create a comprehensive model for decoding continuous motion intentions from sEMG. Mansooreh et al. [23] proposed a compact transformer-based hand gesture classification system to extract motor unit spike trains from high-density sEMG, enhancing classification accuracy. Additionally, a bio-inspired neural network (BNN) was developed to model the information propagation from sEMG to extremity movements, improving recognition accuracy for six wrist movements [24].

This study focused on the impact of electrode locations on limb condition effect and the strategies of mitigating the effect. Myoelectric signals from different locations were collected under both static and dynamic limb conditions. The contribution of this study included: (1) the variation of limb condition effect with the electrode locations from elbow to wrist was explored and the optimal location was selected; (2) multiple-condition training and feature selection strategies were employed and their performance on mitigating limb condition effect was evaluated with different electrode locations. The results of this study would provide valuable insights for the development of wearable human–machine interfaces and the design of more robust and accurate gesture recognition systems.

Methods

Participants

Fourteen healthy, able-bodied subjects are recruited in this study. The details of every subject are shown

in Table 1. All subjects signed the informed consent before the experiment. The experiment procedures were in accordance with the Declaration of Helsinki, and approved by the Research Ethics Committee of West China Hospital (2022-505).

Experimental protocol

Before data collection, the subjects' forearms were cleansed with alcohol to ensure optimal skin condition and reduce signal noise. To investigate the effect of electrode placement in the radial direction, sEMG signals were recorded at three locations: the wrist, the middle of the forearm, and the elbow. At each location, four sEMG sensors (Noraxon Ultium EMG, USA) were positioned equidistantly around the surface of the forearm, as illustrated in Fig. 1. The sampling frequency was set to 2000 Hz. Signals were band-pass filtered between 20 and 500 Hz using a 4th-order Butterworth filter, and a 45–55 Hz band-stop filter was applied to remove power line interference.

Table 1 summary of the details of the subjects

Sub ID	Gender	Age	Dominant hand	Health condition
S1	Male	34	Right	Healthy
S2	Male	27	Right	Healthy
S3	Female	25	Right	Healthy
S4	Male	19	Right	Healthy
S5	Male	29	Right	Healthy
S6	Male	28	Right	Healthy
S7	Male	18	Right	Healthy
S8	Male	19	Right	Healthy
S9	Male	27	Right	Healthy
S10	Male	27	Right	Healthy
S11	Male	25	Right	Healthy
S12	Male	23	Right	Healthy
S13	Male	26	Right	Healthy
S14	Male	25	Right	Healthy

To investigate the effect of limb condition on gesture recognition from myoelectric signals, the following ten limb conditions were considered:

S/AD: the arm was naturally extended toward to ground at the side by facing palm inward (static condition 1).

S/FU: the elbow was flexed to 135∘ in the sagittal plane (static condition 2).

S/AU: the upper arm was raised forward on the horizontal plane (static condition 3).

S/AA: the upper arm was abducted on the horizontal plane (static condition 4).

D/FUDS: the forearm was swung around the elbow joint between S/AD and S/FU slow (1 cycle forth and back in 6 s, dynamic condition 1).

D/FUDF: the forearm was swung around the elbow joint between S/AD and S/FU fast (1 cycle forth and back in 2 s, dynamic condition 2).

D/AUDS: the upper arm was swung around the shoulder joint between S/AD and S/AU slow (1 cycle forth and back in 6 s, dynamic condition 3).

D/AUDF: the upper arm was swung around the shoulder joint between S/AD and S/AU fast (1 cycle forth and back in 2 s, dynamic condition 4).

D/AAAS: the upper arm was swung around the shoulder joint between S/AD and S/AA slow (1 cycle forth and back in 6 s, dynamic condition 5).

D/AAAF: the upper arm was swung around the shoulder joint between S/AD and S/AA fast (1 cycle forth and back in 2 s, dynamic condition 6). These limb motion conditions are showed in Fig. 2. In each limb condition, the subject performed the 7 types of gestures: hand close (HC), hand open (HO), wrist flexion (WF), wrist extension (WE), hand pinch (HP), hand lateral grasp (LG) and rest (RE), as Fig. 3 shows, trial by trial in 10 limb conditions; 5 trials EMG data were collected in each limb condition. Therefore, each subject performed 50 trials in total. Subjects were given two minutes to rest between every two trials to avoid fatigue.

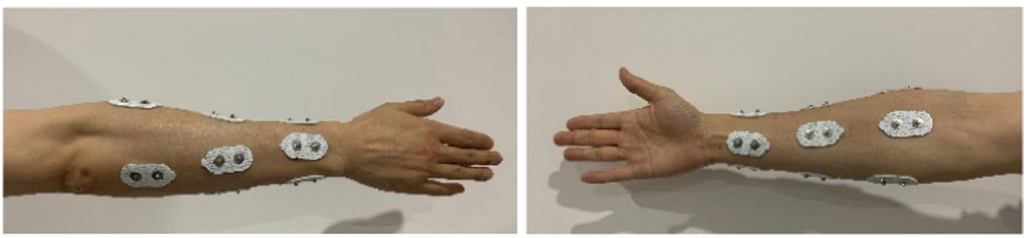

Fig. 1 Placement of the electrodes from the wrist to the elbow photographed from **a** posterior, **b** anterior. Every four electrodes were equidistantly placed around circumference of wrist, mid and elbow in direction parallel to muscle fiber

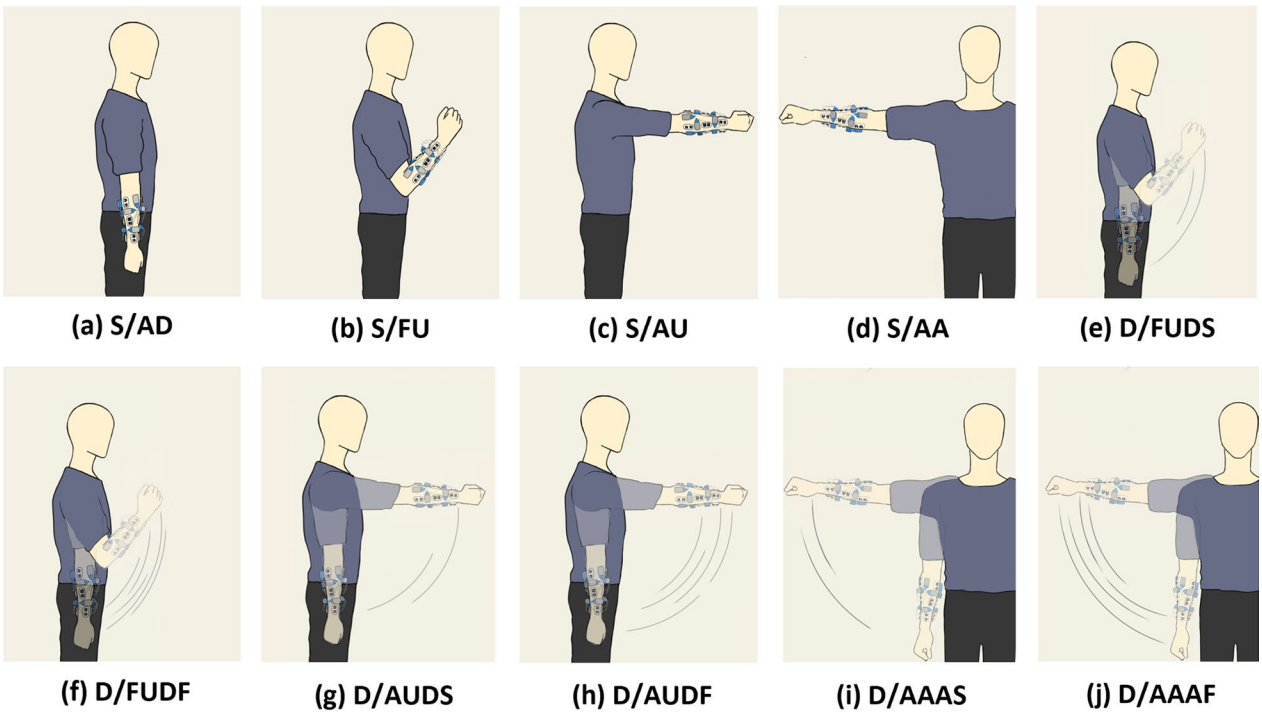

Fig. 2 Limb conditions for EMG acquisition. **a** S/AD: static, arm down (); **b** S/FU: static, forearm up; **c** S/AU: static, arm up; **d** S/AA: static, arm abduction; **e** D/FUDS: dynamic, forearm up and down, slow; **f** D/FUDF: dynamic, forearm up and down, fast; **g** D/AUDS: dynamic, arm up and down, slow; **h** D/AUDF: dynamic, arm up and down, fast; **i** D/AAAS: dynamic, arm abduction and adduction, slow; **j** D/AAAF: dynamic, arm abduction and adduction, fast

Feature extraction

To eliminate the transient states of the gesture EMG, only the central 2 s of data from each movement were used for analysis. The data were segmented into 200 ms windows with a 75% overlap, and sEMG features were extracted from each window. The traditional sEMG feature set, TDAR, was employed in this study, comprising Hudgins time-domain features [25] and six autoregressive coefficients. Linear Discriminant Analysis (LDA) was selected as the classifier due to its extensive use in sEMG-based

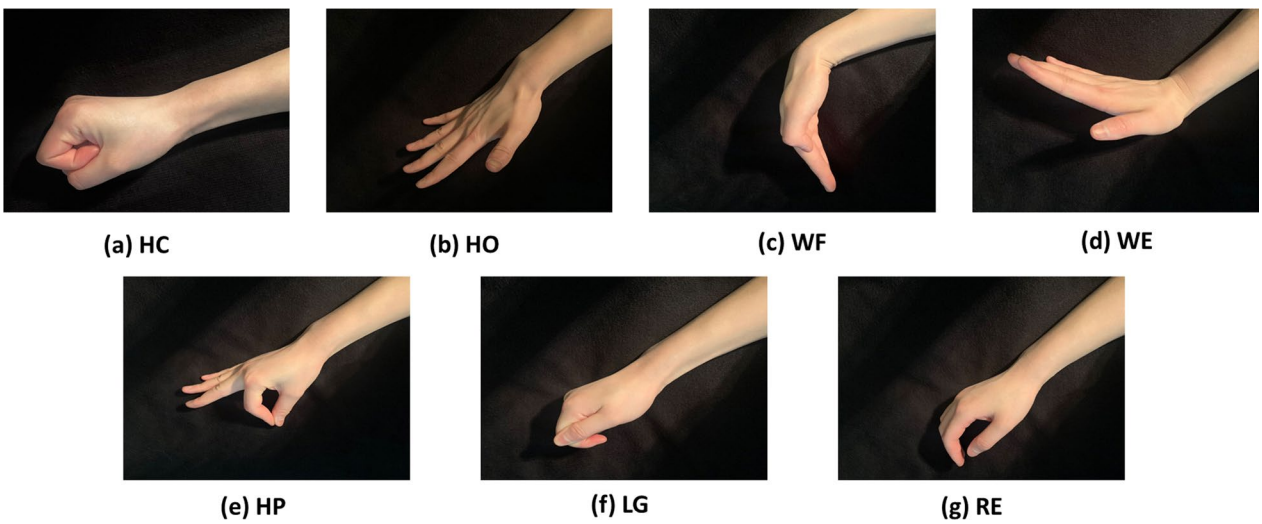

Fig. 3 Gesture classes needed to be classified. **a** Hand close. **b** Hand open. **c** Wrist flexion. **d** Wrist extension. **e** Hand pinch. **f** Lateral grasp. **g** Rest

gesture recognition studies. Previous research has shown that LDA provides performance comparable to more complex classifiers, while requiring significantly less computational time [26]. Consequently, we initially constructed a classifier using LDA to examine the impact of different arm movements on sEMG pattern recognition.

Effect of sEMG acquisition location on sEMG pattern recognition

Given the different sEMG acquisition placements described earlier, we compared the performance of each location on pattern recognition using the separation index (SI). In the pursuit of classification, we assign a class label to an input feature vector derived from the sEMG signal pattern. To achieve this, we construct a hyper-ellipsoid for each class using the centroid (μ) and covariance (S) of the feature vectors. This hyper-ellipsoid is aligned with the principal components of the data, with its semi-principal axes corresponding to the standard deviations of these components, as illustrated in Fig. 4. Our focus is on analyzing variations in the relationships among hyper-ellipsoids under different limb conditions. Specifically, we examine the maximum SI within a single class across 10 different limb conditions and the SI between different classes across the same 10 limb conditions.

SI is formulated to measure interclass distances. We define SI as one-half the Mahalanobis distance from the centroid of the hyper ellipsoid of one group to the centroid of the ellipsoid of the nearest group and average this value across the six active classes (excluding rest).

$$\mathrm{SI}_{wit} = \frac{1}{10}\sum_{j=1}^{10} SI_{wit}(j) \tag{1}$$

$$SI_{wit}(j) = \frac{1}{6}\sum_{i=1}^{6} \max_{k=1,\ldots,j-1,j+1,\ldots,10} \frac{1}{2}\sqrt{(\mu_{ik}-\mu_{ij})^T S_{ij}^{-1}(\mu_{ik}-\mu_{ij})} \tag{2}$$

$$\mathrm{SI}_{bet} = \frac{1}{10}\sum_{j=1}^{10} SI_{bet}(j) \tag{3}$$

$$SI_{bet}(j) = \frac{1}{6}\sum_{i=1}^{6} \min_{\substack{p=j,k=1,\ldots,i-1,i+1,..,6 \\ p\neq j,k=1,2,\ldots,6}} \frac{1}{2}\sqrt{(\mu_{kp}-\mu_{ij})^T S_{ij}^{-1}(\mu_{kp}-\mu_{ij})} \tag{4}$$

where 10 is the number of limb conditions, 6 is the number of gestures without rest condition, S_{ij} is the covariance of limb condition j of class i, μ is respectively the centroid of the one group with the same kind of annotation with S_{ij}.

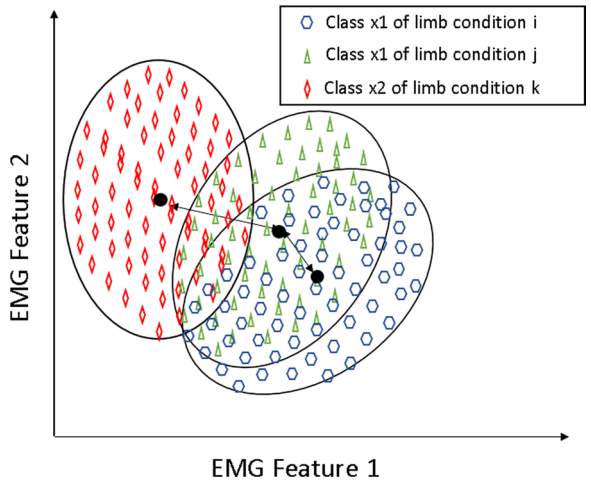

Fig. 4 Illustration of constructing hyper ellipsoids for simulating the feature movement from the change of limb conditions. This figure is just showing bidimensional structure of hyper ellipsoids. And hyper ellipsoids are constructed by centroid (μ) and covariance matrix (S) of feature vectors

Solving effect of arm movements

To address this issue, we proposed a multi-condition classifier using LDA. Arm movements significantly impact motion decoding from sEMG signals, so by training the model with multi-condition data, we aim to develop a more robust model that achieves higher accuracy. Additionally, we employed the sequential forward feature selection (SFFS) algorithm to identify the optimal feature set, further enhancing the accuracy and robustness of the LDA model. Through this approach, we seek to discover a reliable and precise feature set for an effective gesture recognition system. The specific features selected are listed in Table 2.

Statistical analysis

A one-way analysis of variance (ANOVA) was used to assess the statistical significance of variations among the compared instances, which in this study refer to different LDA models, particularly in the evaluation of classification errors. The factors under consideration included both the subject and the case, treated as fixed factors. A significance level of 0.05 was set to determine if significant differences were present.

Table 2 The features to be selected

Type	Order	Feature name	Abbreviation
Time domain feature	0	Mean absolute value	MAV
	1	Variance of EMG	VAR
	2	Root mean square	RMS
	3	Waveform length	WL
	4	Difference absolute standard deviation value	DASDV
	5	Zero crossing	ZC
	6	Myopulse percentage rate	MPR
	7	Willison amplitude	WAMP
	8	Slope sign change	SSC
Frequency domain feature	9	Mean frequency	MNF
	10	Median frequency	MDF
	11	Peak frequency	PKF
	12	Total power	TTP
	13	First spectral moment	SM1
	14	Second spectral moment	SM2
	15	Third spectral moment	SM3
	16	Power spectrum ratio	PSR
	17	Variance of central frequency	VCF
Auto-regressive coefficient	18	1st AR	AR1
	19	2nd AR	AR2
	20	3rd AR	AR3
	21	4th AR	AR4
	22	5th AR	AR5
	23	6th AR	AR6

Results

A. Limb condition effect analysis

(1) Performance comparison among different electrode locations

The average inter-condition and intra-condition classification errors for the three electrode locations were calculated across all subjects and gestures, as shown in Fig. 5. Ten distinct condition-specific classifiers were trained,

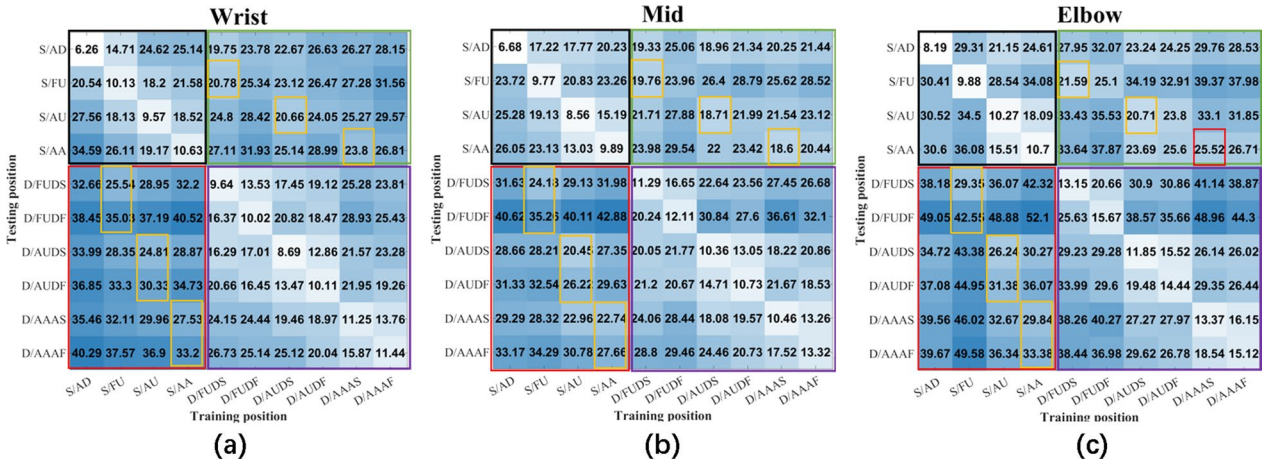

Fig. 5 Confusion matrix of classification errors (in %) averaged across all subjects and all classes when single-condition classifiers (LDA) are used. Darker blue boxes imply greater errors. **a** Wrist sEMG has the best dynamic recognition ability when training in dynamic conditions. **b** Mid sEMG has the best performance of inter-condition. c Elbow sEMG is the worst in all four training and testing conditions

each using data exclusively from one specific limb condition and then tested on data from all limb conditions. The matrix cells represent the average error for all gestures across subjects, with the vertical and horizontal axes indicating the training and testing conditions, respectively. Intra-condition classification errors, shown on the main diagonal, represent errors within the same limb condition, while off-diagonal elements represent inter-condition errors. The mean intra-condition classification errors along the diagonal for three electrode locations were 9.77%, 10.31%, and 12.26%, respectively. The mean inter-condition errors were 25.42%, 24.51%, and 32.14%, respectively. The performance of wrist sEMG and mid sEMG was similar, and they were both better than elbow sEMG.

Figure 6 shows the impact of electrode locations on class-specific outcome. This illustration mirrors the results in Fig. 5, but averages them across limb conditions rather than gestures. Figure 6 shows HO, HP, LG have the lowest accuracy in elbow sEMG while wrist sEMG has the much higher accuracy of HO, HP and LG than the mid of forearm and elbow location. This phenomenon implies that the sEMG signals from wrist location has the best performance of decoding fine movements of fingers. And for mid sEMG, HC, WF and RE have the best performance among the three kinds of sEMG. And it is noteworthy that WE's error rate is much lower than wrist sEMG and almost the same as the best one-elbow sEMG. This phenomenon tells us that the movement of the wrist will influence the sEMG of the wrist and within a certain range, the farther away from the wrist, the better the signal quality, of which the elbow signal quality is the highest. For reliable sEMG-based equipment design, we can select the gestures suitable for different locations of sEMG signals to do the corresponding decoding work. For example, the wrist sEMG is suitable for fine finger movements, the mid and elbow sEMG is better for wrist movements.

To delve deeper into the impact of limb conditions on the discrimination of individual classes, the inter-condition classification matrix presented in Fig. 5, the results have been dissected into class-specific matrices, as depicted in Fig. 7. The gestures that are particularly influenced by limb conditions are evident through darker red-colored elements situated away from the main diagonal. It is displayed that certain conditions worsen the discrimination challenges for these specific classes more than others.

For hand closure (HC), the LDA classifiers trained on static limb conditions performed the worst on all dynamic limb conditions, particularly at the wrist. This indicates that for the hand closure action, sEMG signals at the wrist are significantly affected by dynamic limb conditions, whereas the impact on sEMG signals at the mid forearm and elbow is much smaller. The average recognition error rates for the three areas are 28.38%, 22.36%, and 29.34%, respectively. Additionally, by summing the errors across all testing conditions for each training condition, the best training conditions for the three electrode locations were identified as D/AUDS, D/AAAS, and D/AUDF.

For HO, the wrist sEMG has the best performance with error of 18.89%, while mid sEMG is 24.17%, elbow sEMG is 31.66%. The same as HC, the best training conditions for three electrode locations are S/FU, D/FUDS, D/FUDS.

For WF, the mid sEMG has the best performance with error of 23.69% among these three sEMG electrode locations, while wrist sEMG is 32.35% and elbow sEMG is

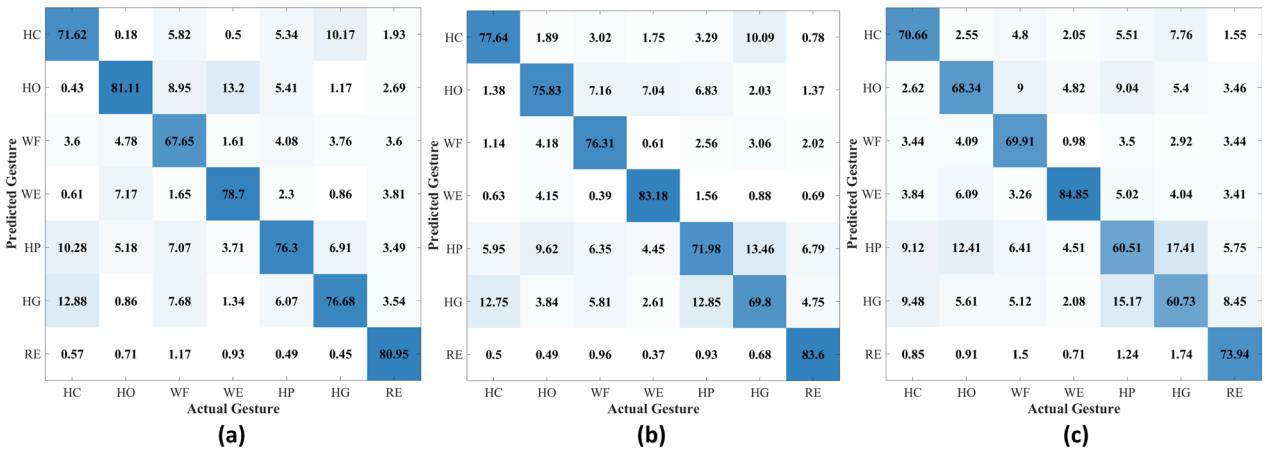

Fig. 6 Confusion matrix of classification error (in %) of gestures averaged across all subjects and all limb conditions. Darker blue boxes imply greater errors. **a** Wrist. **b** Mid. **c** Elbow

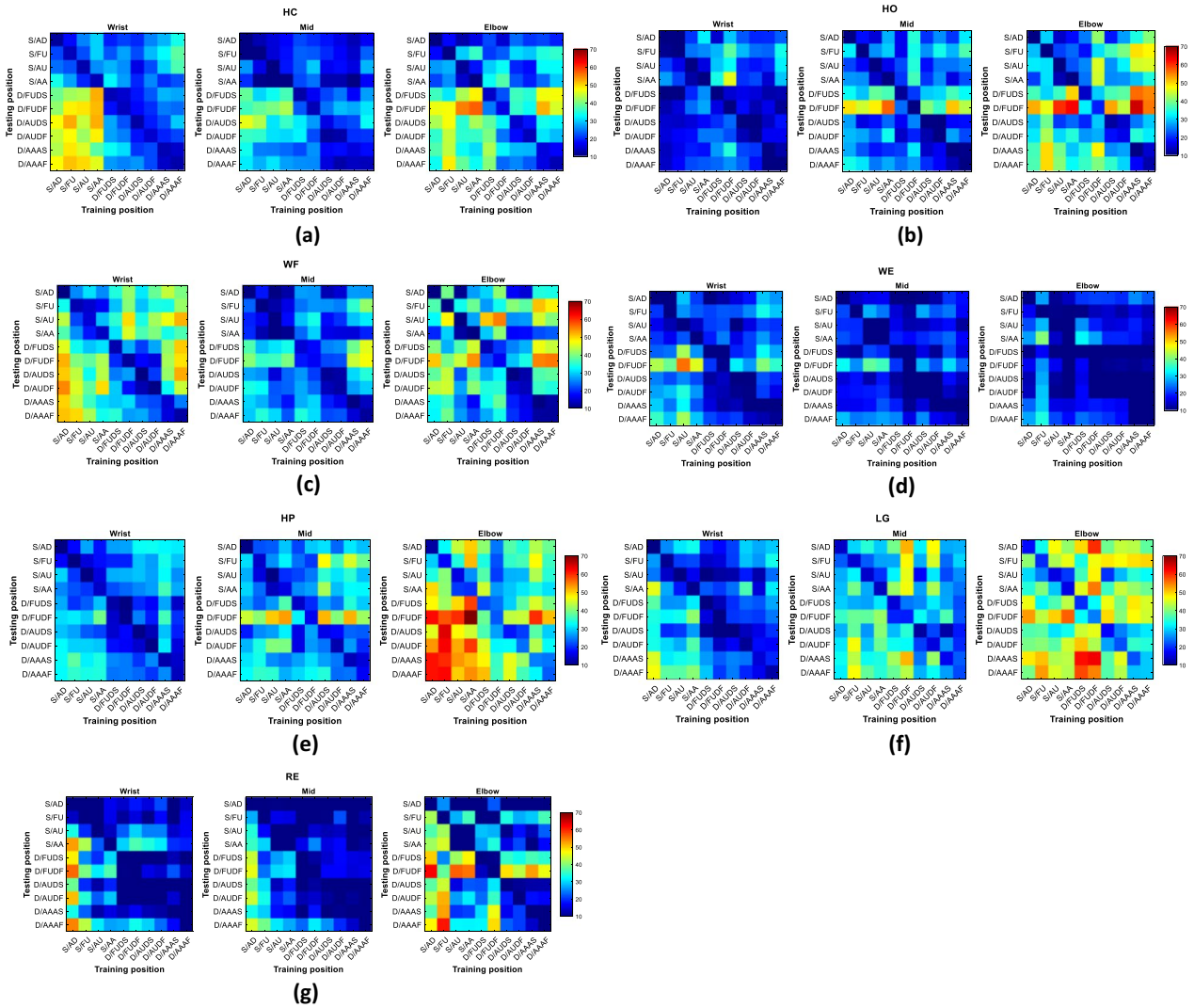

Fig. 7 Confusion matrix of classification errors (in %) averaged across all subjects for each class in three electrode locations: wrist, mid and elbow. Darker red means greater values. **a** HC. **b** HO. **c** WF. **d** WE. **e** HP. **f** LG. **g** RE

30.09%. The best training conditions for three electrode locations are D/AUDS, D/AUDS, D/AUDS.

For WE, the elbow sEMG has the lowest error of 15.15%, the mid sEMG has the error of 16.82% and the wrist sEMG has the highest error of 21.30%. The best training conditions for three electrode locations are D/FUDF, D/FUDF, S/AA.

For HP and LG, the wrist sEMG has the best performance, which indicates that wrist sEMG has the best ability of recognizing the fine hand movements among these three kinds of EMG. The best training conditions for HP in three electrode locations are D/FUDF, D/FUDS, D/FUDF. And the best training conditions for LG in three electrode locations are D/FUDF, D/AAAF, D/AUDS.

For RE, the wrist sEMG has the similar good performance as the mid sEMG, and are much better than elbow EMG. The best training conditions for three electrode locations are D/AAAF, D/AAAS, D/FUDS.

(2) Comparison between dynamic and static limb conditions

Further, the matrix in Fig. 5 was divided in four blocks, which included different training and testing combinations. Among them, black parts mean training in

static limb conditions and testing in static limb conditions, red parts mean training in static limb conditions and testing in dynamic limb conditions, green parts mean training in dynamic limb conditions and testing in static limb conditions, and purple parts mean training in dynamic limb conditions and testing in dynamic limb conditions. The averages of these four blocks in three electrode locations were 19.09%, 33.12%, 25.76%, 18.52% vs 17.48%, 30.39%, 23.02%, 20.77% vs 23.28%, 38.74%, 29.52%, 27.90%.

By observing the limb conditions carefully, some similarity between different conditions can be found. The dynamic conditions can be seen as some combinations of different static conditions. For example, dynamic condition D/FUD can be seen as the combination of static conditions S/AD and S/FU. D/AUD can be seen as the combination of S/AD and S/AU. D/AAA can be seen as the combination of S/AD and S/AA. The hypothesis is that the similarity of the condition can lead to the similarity of performance. In fact, for wrist sEMG, the recognition accuracy of each dynamic condition has the relationship with the related static conditions. The numbers in the small yellow boxes represent the classification results of the classifiers trained for the limb condition represented by this column. These classifiers perform best among the static or dynamic classifiers to which this column belongs when classifying the limb conditions represented by this row. This fact indicates that limb conditions with certain similarity in form play a role in enhancing the robustness of sEMG pattern recognition. In other words, sEMG signals corresponding to the same gestures of these limb conditions exhibit a higher correlation than signals from other limb conditions. It is noteworthy that the classifier trained in the fast limb conditions does not exhibit the same distinct advantage over the relative static limb conditions as the classifier trained in the slow dynamic limb conditions. A similar phenomenon can be observed in the middle forearm and the elbow, except for one test in the elbow which is not as expected (the corresponding area is marked in a small red box in Fig. 5), but it is very close to the best. This phenomenon indicts that dynamic limb conditions' sEMG can include the information of related static limb conditions' sEMG. And vice versa, static limb conditions also can include the information of the related transient conditions of dynamic conditions. This phenomenon also inspires us to design some complex dynamic limb conditions to cover more usual and normal static limb conditions we usually show in daily life to include more diverse sEMG information. This operation can improve the robustness of recognition models.

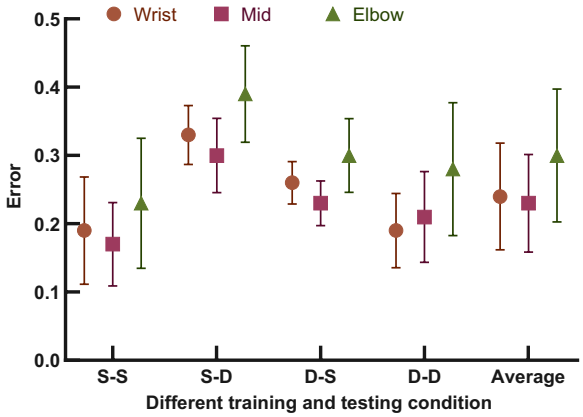

Fig. 8 The error rate of different training and testing conditions,'S' represents static limb conditions, 'D' represents dynamic limb conditions. The character before dash means training limb condition, the character after dash means testing condition

From Fig. 8, wrist sEMG has the best performance in dynamic training and dynamic testing. This is very suitable for the wearable equipment's design. Because the application scenarios of the wearable equipment are almost dynamic. This phenomenon demonstrates the feasibility of wrist sEMG in complicated real world. And by observing the other three groups, the gap between the wrist sEMG and mid sEMG is not large while much better than elbow sEMG.

(3) Effect of moving speed in dynamic limb conditions

To analyze the influence of different speeds in dynamic limb conditions, Fig. 9 presents the recognition error rates for various dynamic limb conditions at different speeds. Fast and slow conditions of the same type are positioned adjacently. For sEMG at all three locations, ANOVA results indicate no significant difference between fast and slow dynamic conditions in terms of the robustness of a model trained under these conditions and tested across all limb conditions (including static conditions).

In real applications of limb-based sEMG wearables, dynamic conditions are usual. By observing the two kinds of dynamic testing groups, the phenomenon which is that wrist sEMG has the lowest average error of six dynamic condition training models illustrates that wrist sEMG is very suitable for the real applications of human–machine interface.

(4) Feature space analysis

As shown in Fig. 10, wrist sEMG demonstrates the best separation of seven different gestures across 10 limb conditions compared to the other two locations.

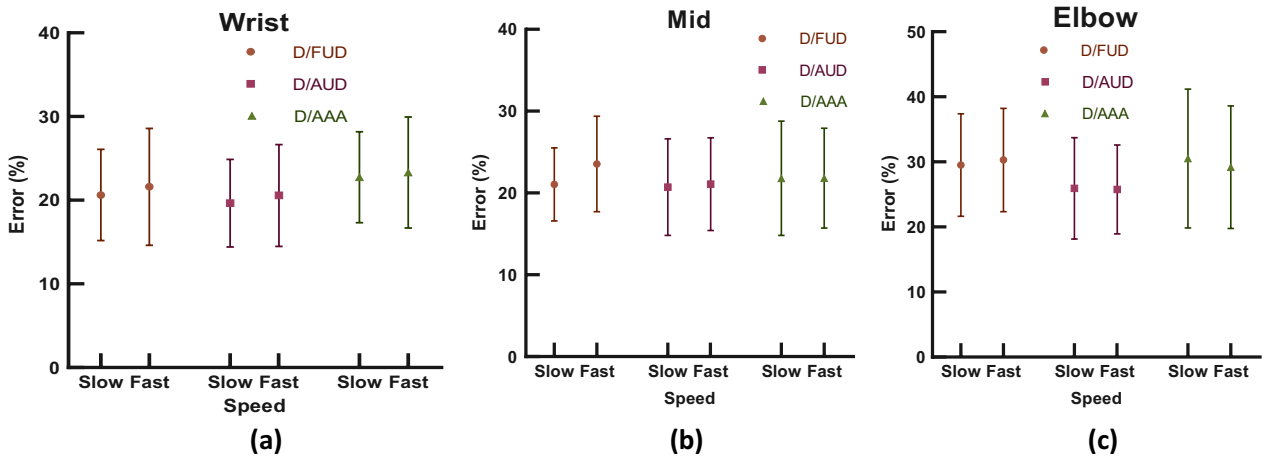

Fig. 9 The comparison of the influence of different speeds for different dynamic limb conditions on gesture recognition. Every result is achieved by one LDA model which is trained in the represented dynamic limb condition and tested in all ten limb conditions. **a** Wrist. **b** Mid. **c** Elbow

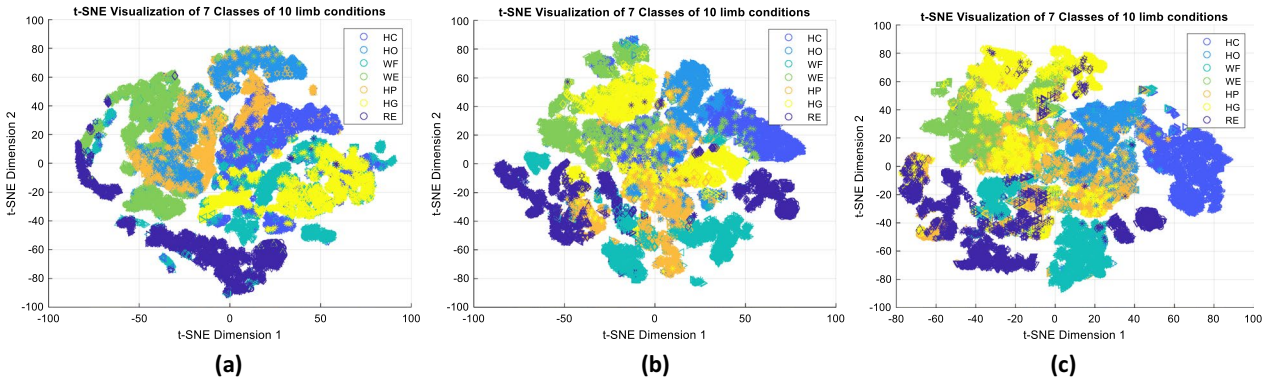

Fig. 10 Visualization of different class of different limb conditions. A very obvious phenomenon can be found in three subfigures which is the wrist EMG has the best separability of seven gestures while the elbow EMG is the worst. **a** Wrist. **b** Mid. **c** Elbow

Figure 11 illustrates the average SI within-class and between-class across 14 subjects, indicating that wrist sEMG offers the best overall performance in the recognition task. ANOVA results reveal a significant difference ($p = 0.026$) in within-class SI among the wrist, mid, and elbow locations, with wrist and mid sEMG showing similar values, both lower than the elbow. For between-class SI, wrist sEMG has the highest value, indicating the best discrimination of different gestures at this location.

B. Strategies comparison for mitigating the limb condition effect

(1) Multiple-condition training

The average classification errors of using data from single and multiple (2–5) conditions in the training dataset and all ten conditions in the test dataset were calculated and are presented in Fig. 12. First, we can find that the recognition errors decreased with the number of training conditions increasing. This phenomenon is common in three sEMG electrode locations. And the best combinations for each group are showed in the table below each figure. We can find D/AAAF is the best training condition for single-condition training. It implies the fast swinging around the shoulder joint between S/AD and S/AA has the most information diversity than other 9 limb conditions. But with the computation continues, the best feature sequences for three electrode locations begin to be different. By careful observation, the inner law of the choice of the added feature is clear. It is that cover as more important limb conditions as possible. Through ANOVA method, we can find that each group is significantly different with adjacent groups of three sEMG electrode locations by the p-values less than 0.05. And we can find that each group's best performance and its combination in Table 3.

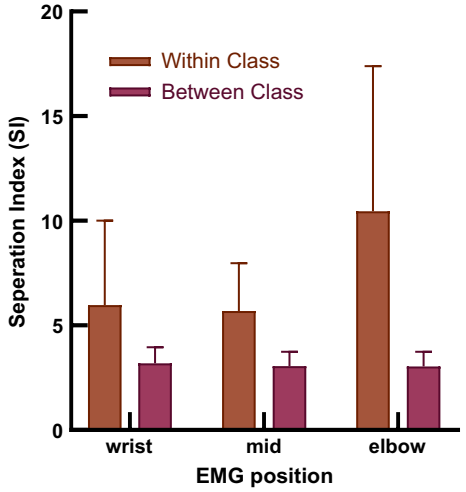

Fig. 11 Feature Space Analysis: SI – within class distance for same gesture vs. Interclass distance among different gestures. Bars represent value calculated by formula (1)-(4), and standard deviation is computed over the values

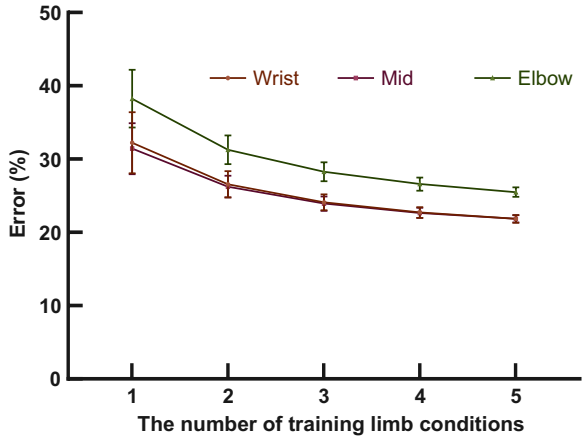

Fig. 12 Classification errors when training in each combination of limb condition subsets and testing in all ten limb conditions. The reduction speed of classification errors is much slower after four limb conditions. Wrist sEMG and mid sEMG are much better than elbow sEMG

(2) Feature optimization

To develop a more efficient and convenient method for training a robust and accurate pattern recognition system, we employed the sequential forward feature selection (SFFS) method to create a higher-quality feature set for gesture recognition. Within the feature space, we selected three types of signal features: time domain features, frequency domain features, and autoregressive coefficients. These features encompass nearly all key elements used in reliable sEMG-based recognition systems.

For achieving the best feature set for three different sEMG electrode locations, we apply SFFS method on them. Firstly, we run the codes on wrist sEMG and after 16 iterations, we get the best feature sequence for wrist sEMG. The numerical sequence is [4, 2, 15, 3, 8, 6, 7, 10, 0, 23, 22, 19, 21, 18, 20, 16], which can be translated to [DASDV, RMS, SM3, WL, SSC, MPR, WAMP, MDF, MAV, AR6, AR5, AR2, AR4, AR1, AR3, PSR]. Then we run the similar codes on middle location and elbow location to get their best feature sets. They are [3, 0, 14, 4, 8, 6, 7, 10, 9, 5, 1, 17, 18, 19, 23, 22, 21] and [3, 0, 14, 6, 4, 8, 7, 13, 2, 11], respectively after 17 and 10 circles, which can be translated to [WL, MAV, SM2, DASDV, SSC, MPR, WAMP, MDF, MNF, ZC, VAR, VCF, AR1, AR2, AR6, AR5, AR4] and [WL, MAV, SM2, MPR, DASDV, SSC, WAMP, SM1, RMS, PKF].And the best accuracy of wrist, middle and elbow are 81.02%, 80.35% and 72.86%. And every iteration's accuracy of three sEMG are showed in Fig. 13. For more details, we get the related confusion matrix of ten different limb conditions of wrist, middle and elbow, showed in Fig. 14. By checking the three matrices, we can find that although SFFS algorithm can find a better feature set to improve the accuracy of three sEMG locations' pattern recognition performance, it still cannot solve some limb conditions' low robustness like S/FU, D/FUDS, D/AUDF.

As the number of features increases, the improvement in accuracy becomes progressively smaller. Using the t-test, we calculated the significance of accuracy differences across various feature sets. For wrist sEMG, the accuracy in the fifth cycle (78.85%) shows a significant improvement over the fourth feature set, with a p-value of 0.035. For mid sEMG, the fourth feature set (76.15%) significantly improves accuracy compared to the third, with a p-value of 0.014. For elbow sEMG, the third feature set's accuracy (69.95%) shows a significant improvement over the second, with a p-value of less than 0.001.

Disscussion

The primary aim of this paper is to conduct a comprehensive and systematic investigation into the influence of limb conditions and sEMG electrode locations on pattern recognition tasks. The results demonstrate that wrist sEMG outperforms middle and elbow sEMG in gesture recognition across multiple dimensions. Additionally, we propose several strategies to enhance the performance of inter-condition gesture recognition systems, thereby improving the robustness of the classifier.

Table 3 The best effect of combination of different training limb conditions

Location	Number of training	Average error (%)	Min error (%)	Best combination
Wrist	1	32.23	24.88	D/AAAF
	2	26.57	24.52	S/AA, D/FUDF
	3	24.10	22.36	S/FU, D/AUDS, D/AAAF
	4	22.72	21.40	S/FU, D/FUDF, D/AUDS, D/AAAF
	5	21.85	20.72	S/FU, S/AA, D/FUDF, D/AUDS, D/AAAF
Mid	1	31.42	23.21	D/AAAF
	2	26.24	24.33	D/FUDS, D/AAAF
	3	23.92	22.27	S/AU, D/FUDF, D/AAAF
	4	22.65	21.50	S/AU, D/FUDS, D/FUDF, D/AAAF
	5	21.85	20.99	S/AU, D/FUDS, D/FUDF, D/AUDS, D/AAAF
Elbow	1	38.24	30.95	D/AAAF
	2	31.27	28.82	D/FUDF, D/AAAS
	3	28.28	25.88	S/AU, D/FUDF, D/AAAF
	4	26.58	25.03	S/AU, D/FUDF, D/AUDS, D/AAAF
	5	25.50	24.34	S/FU, S/AA, D/FUDF, D/AUDS, D/AAAF

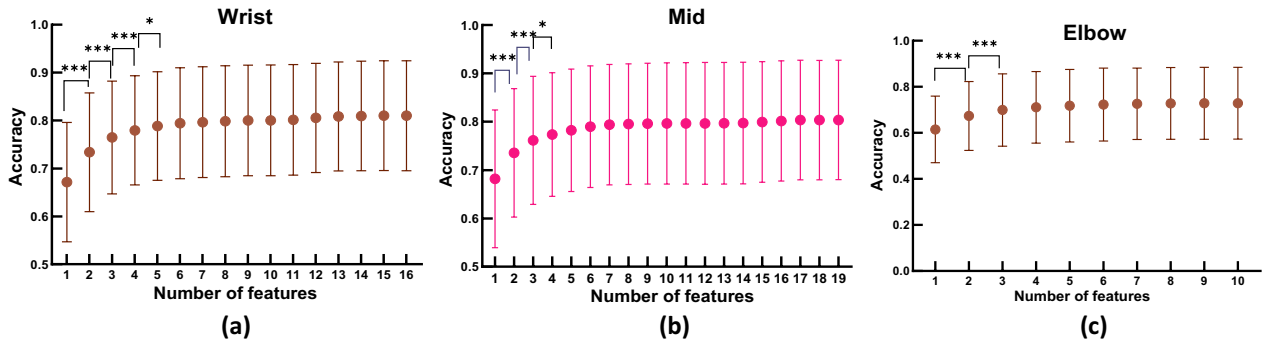

Fig. 13 The iteration procedure of classification accuracy in three sEMG electrode locations. Each data point is equivalent to averaging all test results from 14 subjects (the model obtained after each person is trained on one limb condition data needs to be averaged across all 10 limb conditions, for a total of 100 possible choices). **a** Wrist. **b** Mid. **c** Elbow

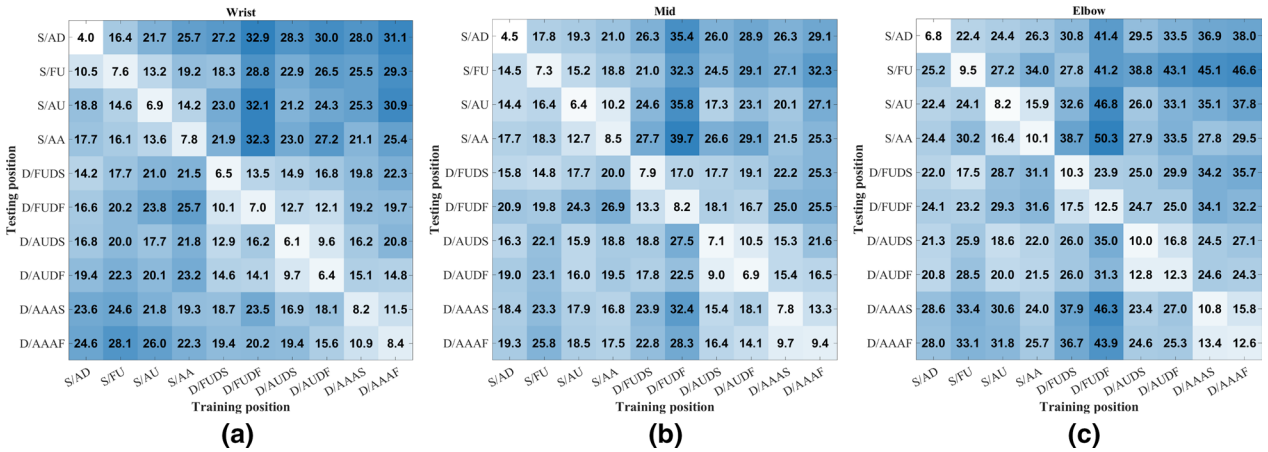

Fig. 14 The confusion matrix of classification errors of the best feature set on three sEMG electrode locations. For wrist, it is the result of the 16th iteration. For mid, it is the result of the 17th iteration. For elbow, it is the result of 10th iteration. **a** Wrist. **b** Mid. **c** Elbow

A. Limb condition effect analysis

(1) Performance comparison among different electrode locations

In this paper, we use various indexes and methods to evaluate the performance of sEMG at different locations. The separation index (SI) reveals that wrist sEMG has similar within-class separability to mid-forearm sEMG, both of which are significantly better than elbow sEMG. For between-class separability, wrist sEMG shows the highest value among the three locations, indicating superior discrimination of different gestures numerically. Additionally, t-SNE visualizations confirm that wrist sEMG provides the best class separability across different limb conditions. These two metrics demonstrate that wrist sEMG is the most effective choice for gesture recognition from both numerical and visual perspectives. This superiority is further supported by additional testing results, including single-limb condition training, multiple-limb condition training, and the deployment of the SFFS method.

(2) Performance comparison between static and dynamic conditions

Firstly, training under different limb conditions reveals that some conditions perform better for gesture recognition tasks, while others are less effective. Analysis of the testing results indicates that S/AD is the optimal limb condition for both training and testing in intra-condition scenarios. This suggests that using data from S/AD and applying the trained model within the same condition yields excellent results. Conversely, since prosthetic hand users encounter various limb conditions in daily life, we calculated the average accuracy of models trained under different limb conditions. We found that D/AUDS achieved the best average performance across ten limb conditions for wrist and mid-forearm sEMG, and second-best performance for elbow sEMG, closely matching the top result. The average accuracies of D/AUDS at the three electrode locations are 19.66%, 20.72%, and 25.95%, respectively. These findings indicate that D/AUDS is the best choice for single-limb condition training in complex usage scenarios. Additionally, the results demonstrate that slow dynamic movements are more effective than fast dynamic movements for improving model robustness.

Upon careful observation, we note that D/FUD combines elements from S/AD and S/FU. It is hypothesized that sEMG data from D/FUD may have some correlation with both S/AD and S/FU. Similarly, D/AUD combines S/AD and S/AU, while D/AAA combines S/AD and S/AA. Analysis of the matrices for the three EMG acquisition configurations reveals that classifiers trained on related slow dynamic limb conditions show superior recognition accuracy for some static limb conditions. Conversely, some dynamic limb conditions exhibit similar trends when trained with related static conditions. This suggests that incorporating more static limb conditions at slow speeds into dynamic training can enhance the robustness of the classifier across various limb conditions.

B. Solutions

In this research, we examined the performance of three different electrode locations on the forearm for sEMG pattern recognition tasks. We employed three distinct methods to assess the impact of each electrode location. In LDA single-limb condition training, we found that wrist sEMG achieves accuracy similar to that of mid-forearm sEMG. To enhance model accuracy, we utilized multiple limb conditions for training, which proved to be highly effective in improving model robustness. This result is expected and aligns with standard practice. However, for practical applications, a convenient and simple training protocol is desirable. Therefore, we aimed to use as few limb conditions as possible for data acquisition while still achieving satisfactory performance.

Our analysis reveals that a four-limb-condition training scheme is optimal for the training dataset. Beyond four limb conditions, adding more does not significantly improve accuracy. Notably, the three four-limb-condition training schemes proposed in this research all include a higher proportion of dynamic conditions compared to static ones. This suggests that dynamic conditions capture more movement information in sEMG signals. For time-constrained scenarios where recording different limb conditions is limited, prioritizing dynamic conditions is advisable. Additionally, if the training process is restricted, selecting a few fixed combinations of limb conditions can be effective. The table provides concrete recommendations for practitioners to develop a more robust recognition system based on these findings.

Through multiple limb condition training, we observed an improvement in model performance. To further enhance the performance of single-limb condition models, we employed the sequential forward feature selection (SFFS) method. This approach significantly improved the performance of the single-limb condition models. We believe that using the selected feature set in combination with multiple limb conditions will yield better results compared to using only the TDAR feature set.

Analysis of the selected features revealed that the initial features are predominantly time-domain features, with many autoregressive indexes also included. Since autoregressive features are a subset of time-domain features, this suggests that time-domain features contribute significantly to better recognition performance. For practical

applications, we recommend using time-domain features for gesture recognition.

Using the t-test method, we identified feature sets with significant improvements during the selection process: [DASDV, RMS, SM3, WL, SSC] for wrist, [WL, MAV, SM2, DASDV] for mid-forearm, and [WL, MAV, SM2] for elbow. The recognition errors for these feature sets are 21.15%, 23.85%, and 30.05%, respectively.

Both methods have their respective advantages and disadvantages. Multi-condition training requires data from many different limb conditions to train a more robust model, which can be time-consuming. On the other hand, the sequential forward feature selection (SFFS) method needs to be run for each individual to determine the optimal feature set, which also requires significant computation time. However, advancements in computer technology have greatly improved computational speed.

For wrist sEMG, a feature set comprising five features can achieve similar performance to that obtained with four limb conditions, demonstrating that the feature selection method can be more efficient in improving model performance compared to multi-condition training.

C. Limitations

This research investigated the limb condition effect on different electrode rings from the elbow to the wrist, and provided the optimal limb condition combination and feature sets for mitigating the effect. However, there were several limitations. As the data of each gesture was collected under ten limb conditions, only seven gestures were involved in this study for reducing the time of data acquisition. As the size of the sensor, the setup of four electrodes and three rings was adopted for the limited space in the forearm. The performance with more gestures and electrodes, such as the high-density grids, should be investigated in future. With the advanced processing methods and more electrodes, the classification accuracy would be increased, but the trend should be the same for the methods used in this study was not specifically designed for any condition. Besides, though group training was simple and effective in reducing limb condition effect, its time consuming and the performance would be plateaued with the addition of limb conditions in training. For improving the robustness further, it was suggested that the combination of the feature selection and group training, with the employment of deep learning methods for its generality ability, might be better than the employment of the single strategies. Finally, this study focused on the steady state part of sEMG signals, which was the same as most myoelectric control studies [27, 28]. For practical applications, transient part was avoidable, and would be investigated in future.

Conclusion

In this paper, we investigate the impact of three sEMG acquisition locations and ten limb conditions on the performance of gesture recognition systems. The results demonstrate that wrist EMG excels in recognizing fine hand gestures, making it ideal for wearable wrist devices. Mid-forearm EMG performs slightly worse than wrist EMG, while elbow sEMG shows the least effectiveness for this task.

To address the issue of weak robustness, we propose two solutions. First, multi-limb condition training significantly improves recognition accuracy for wrist sEMG by approximately 10 percent. We also introduce a new training approach that incorporates more static limb conditions to enhance robustness. Additionally, we applied the sequential forward feature selection (SFFS) method to identify the optimal feature combinations for different sEMG acquisition locations. This method notably enhances the robustness of single-limb condition training models.

This study paves the way for improving the robustness of wrist-based sEMG wearables, offering valuable insights for future development.

Acknowledgements

The authors would like to present their gratitude to all the volunteers who participated in this study.

Author contributions

Jiayuan He and Na Li implemented the experimental protocol and conducted the experiments. Hai Wang and Jiayuan He designed the study and interpreted the results. Hai Wang was in charge of the implementation of signal processing and machine learning methods and the analysis of the data. Hai Wang and Jiayuan He wrote the manuscript. Xiaoyao Gao drawed the illustration figures in the Methods. All authors read and approved the final manuscript.

Funding

This work was supported in part by the Fundamental Research Funds for the Central Universities under Grant YJ202373, in part by the Science and Technology Major Project of Tibetan Autonomous Region of China under Grant XZ202201ZD0001G, in part by the 1.3.5 Project for Disciplines of 1435 Excellence Grant from the West China Hospital under Grant ZYYC22001, and in part by the Key Project from the Med-X Center for Manufacturing under Grant 0040206107007.

Availability of data and materials

Data is provided within the manuscript or supplementary information files.

Declarations

Ethics approval and consent to participate

All subjects signed an informed consent before the experiment, and the experimental procedures were approved by the Research Ethics Committee of West China Hospital, Sichuan University under Application No. 2022-505, and performed in line with the Declaration of Helsinki.

Consent for publication

Not applicable.

Competing interests

The authors declare no competing interests.

Received: 8 March 2024 Accepted: 6 September 2024
Published online: 03 October 2024

References

1. Jiang N, Chen C, He J, Meng J, Pan L, Su S, et al. Bio-robotics research for non-invasive myoelectric neural interfaces for upper-limb prosthetic control: a 10-year perspective review. Natl Sci Rev. 2023;10(5):nwad048.
2. Farina D, Jiang N, Rehbaum H, Holobar A, Graimann B, Dietl H, et al. The extraction of neural information from the surface EMG for the control of upper-limb prostheses: emerging avenues and challenges. IEEE Trans Neural Syst Rehabil Eng. 2014;22(4):797–809.
3. Roche AD, Rehbaum H, Farina D, Aszmann OC. Prosthetic myoelectric control strategies: a clinical perspective. Curr Surg Rep. 2014. https://doi.org/10.1007/s40137-013-0044-8.
4. He J, Zhang D, Jiang N, Sheng X, Farina D, Zhu X. User adaptation in long-term, open-loop myoelectric training: implications for EMG pattern recognition in prosthesis control. J Neural Eng. 2015;12(4):046005.
5. Fougner A, Scheme E, Chan ADC, Englehart K, Stavdahl O. Resolving the limb position effect in myoelectric pattern recognition. IEEE Trans Neural Syst Rehabil Eng. 2011;19(6):644–51.
6. Geng YJ, Zhou P, Li GL. Toward attenuating the impact of arm positions on electromyography pattern-recognition based motion classification in transradial amputees. J Neuroeng Rehabil. 2012. https://doi.org/10.1186/1743-0003-9-74.
7. Liu J, Zhang D, Sheng X, Zhu X. Quantification and solutions of arm movements effect on sEMG pattern recognition. Biomed Signal Proces. 2014;13:189–97.
8. He J, Niu X, Zhao P, Lin C, Jiang N. From forearm to wrist: deep learning for surface electromyography-based gesture recognition. IEEE Trans Neural Syst Rehabil Eng. 2023. https://doi.org/10.1109/TNSRE.2023.3341220.
9. Botros FS, Phinyomark A, Scheme EJ. Electromyography-based gesture recognition: is it time to change focus from the forearm to the wrist? Ieee T Ind Inform. 2022;18(1):174–84.
10. Islam MJ, Ahmad S, Ferdousi A, Haque F, Reaz MBI, Bhuiyan MAS, et al. Optimizing electrode positions on forearm to increase SNR and myoelectric pattern recognition performance. Eng Appl Artif Intel. 2023;122:106160.
11. Pan TY, Tsai WL, Chang CY, Yeh CW, Hu MC. A hierarchical hand gesture recognition framework for sports referee training-based EMG and accelerometer sensors. Ieee T Cybernetics. 2022;52(5):3172–83.
12. Vásconez JP, López LIB, Caraguay ALV, Cruz PJ, Alvarez R, Benalcázar ME. A hand gesture recognition system using emg and reinforcement learning: a Q-learning approach. In: Farkaš I, Masulli P, Otte S, Wermter S, editors. Artificial neural networks and machine learning - Icann 2021, Pt Iv. Cham: Springer International Publishing; 2021. p. 580–91.
13. Yamanoi Y, Ogiri Y, Kato R. EMG-based posture classification using a convolutional neural network for a myoelectric hand. Biomed Signal Process. 2020;55:101574.
14. Scheme EJ, Englehart KB, Hudgins BS. Selective classification for improved robustness of myoelectric control under nonideal conditions. IEEE Trans Biomed Eng. 2011;58(6):1698–705.
15. Kawaguchi J, Yoshimoto S, Kuroda Y, Oshiro O. Estimation of finger joint angles based on electromechanical sensing of wrist shape. IEEE Trans Neural Syst Rehabil Eng. 2017;25(9):1409–18.
16. Xiloyannis M, Gavriel C, Thomik AAC, Faisal AA. Gaussian process autoregression for simultaneous proportional multi-modal prosthetic control with natural hand kinematics. IEEE Trans Neural Syst Rehabil Eng. 2017;25(10):1785–801.
17. Ngeo JG, Tamei T, Shibata T. Continuous and simultaneous estimation of finger kinematics using inputs from an EMG-to-muscle activation model. J Neuroeng Rehabil. 2014. https://doi.org/10.1186/1743-0003-11-122.
18. Wang H, Tao Q, Zhang X. Ensemble learning method for the continuous decoding of hand joint angles. Sensors. 2024;24(2):660.
19. Wen Y, Kim SJ, Avrillon S, Levine JT, Hug F, Pons JL. A deep CNN framework for neural drive estimation from HD-EMG across contraction intensities and joint angles. IEEE Trans Neural Syst Rehabil Eng. 2022;30:2950–9.
20. Hai W, Qing T, Na S, Xiaodong Z. Simultaneous estimation of hand joints' angles toward sEMG-driven human-robot interaction. Ieee Access. 2022;10:109385–94.
21. Ameri A, Akhaee MA, Scheme E, Englehart K. A deep transfer learning approach to reducing the effect of electrode shift in EMG pattern recognition-based control. IEEE Trans Neural Syst Rehabil Eng. 2020;28(2):370–9.
22. Bao TZ, Zaidi SAR, Xie SQ, Yang PF, Zhang ZQ. A CNN-LSTM hybrid model for wrist kinematics estimation using surface electromyography. IEEE Trans Instrum Meas. 2021;70:1.
23. Montazerin M, Rahimian E, Naderkhani F, Atashzar SF, Yanushkevich S, Mohammadi A. Transformer-based hand gesture recognition from instantaneous to fused neural decomposition of high-density EMG signals. Sci Rep. 2023. https://doi.org/10.1038/s41598-023-36490-w.
24. Fang YF, Yang JN, Zhou DL, Ju ZJ. Modelling EMG driven wrist movements using a bio-inspired neural network. Neurocomputing. 2022;470:89–98.
25. Hudgins B, Parker P, Scott RN. A new strategy for multifunction myoelectric control. IEEE Trans Biomed Eng. 1993;40(1):82–94.
26. Bunderson NE, Kuiken TA. Quantification of feature space changes with experience during electromyogram pattern recognition control. IEEE Trans Neural Syst Rehabil Eng. 2012;20(3):239–46.
27. Cote-Allard U, Fall CL, Drouin A, Campeau-Lecours A, Gosselin C, Glette K, et al. Deep learning for electromyographic hand gesture signal classification using transfer learning. IEEE Trans Neural Syst Rehabil Eng. 2019;27(4):760–71.
28. Qi JX, Jiang GZ, Li GF, Sun Y, Tao B. Surface EMG hand gesture recognition system based on PCA and GRNN. Neural Comput Appl. 2020;32(10):6343–51.

Publisher's Note